A comparative study of autokeratometric and Scheimpflug keratometric measurements of the anterior corneal surface: results for a single subject[*]

SD Mathebula[†] and A Rubin[‡]

[†]Department of Optometry, University of Limpopo, Private Bag x1106, Sovenga, 0727 South Africa, and
[‡]Optometric Science Research Group, Department of Optometry, APK, University of Johannesburg, PO Box 524, Auckland Park, 2006 South Africa

[†]<solanim@ul.ac.za>
[‡]<arubin@uj.ac.za>

Abstract

One purpose of the broader study was to determine whether keratometric measurements obtained with an autokeratometer (Nidek ARK-700) would be comparable with those measured using the Oculus Pentacam (model 70700). Ten healthy subjects without ocular abnormality, no previous or current contact lens wear or history of ocular surgery were recruited and at least 43 successive keratometric measurements were obtained for the right eye of each subject using both instruments, namely the autokeratometer and the Pentacam. This paper will concern itself with data from only one of the ten subjects involved, namely Subject 1. The corneal powers were analyzed using multivariate methods for analyzing dioptric power. Scatter plots and meridional profiles of skewness and kurtosis were used to compare the results for the two instruments. Mean dioptric powers in conventional and scientific notation were determined.

The results for this subject indicated that there was a statistically significant difference between the autokeratometry and the Pentacam. Although the means between the two instruments were found to be significantly different at a 95% level of confidence, there was minimal clinical difference between the means of the two instruments. That is, this preliminary investigation suggests that in normal eyes, clinically, keratometric results obtained by means of an autokeratometer and a Pentacam are reasonably similar and can be used interchangeably.

Key words: Scheimpflug photography, Pentacam, keratometry, autokeratometry, corneal power and topography

Introduction

The anterior surface of the cornea is an important refracting component of the eye and commonly is the major source of ocular antistigmatism.[1-4] Several methods of measuring the corneal shape have been used previously. Probably the most common clinical instrument is the manual keratometer that assumes the cornea to be a convex mirror. The modern autokeratometer focuses the reflected corneal image onto an electronic photosensitive device, which instantly records the reflected image and its size and other characteristics and then computes the radius of curvature (and indirectly the power). However, the keratometer has the limitation of measuring corneal shape from only two points approximately 3 mm apart.[1] It cannot measure the dioptric power of the cornea because it measures only the radius of curvature of the corneal front surface and makes an assumption of an artificial value for the index (1.3375) of the cornea to

account for the posterior corneal surface power. This assumption can lead to serious errors in some clinical situations. Because of various factors, in this study an autokeratometer was used in preference to the manual keratometer. Autokeratometers have become increasingly common in both clinical and research settings because they are easy-to-use and accurate instruments requiring less time to operate than manual keratometers.

The Pentacam[5] (model 70700; Oculus, Wetzlar, Germany) is a novel imaging device that uses a rotating Scheimpflug camera and a harmless, ultraviolet-free monochromatic slit light source (blue LED at 475 nm) that rotate together around the optic axis of the eye. Within two seconds, the system rotates 180^0 and generates reconstructions of the anterior eye segment from 12 to 50 slit images (depending on the researcher's preference) that each contain 500 measurements for points on the front and back corneal surfaces. It is a noncontact instrument, which conveniently provides topography maps of the anterior and posterior corneal surfaces. The instrument calculates the refractive power of both surfaces and adds them together to provide a true net power map. Other parameters, such as corneal thickness, are available and can be represented.

The manufacturer[5] claims an accuracy and reproducibility of 1μm (that is, 0.001 mm) for this instrument. Initial publications[6-12] have reported excellent repeatability with measurements of central corneal thickness and anterior chamber depth measurements.

However, when a new instrument is brought into clinical practice, it is important to compare it to well-established methods to validate it. Little appears to be known as to whether the results for these two methods (autokeratometry and the Pentacam) are comparable and whether the two instruments can be used interchangeably. The main purpose of this paper was to compare the shape of the anterior corneal surface obtained with the Pentacam to that obtained with the Nidek 700 autokeratometer.

Methods

Ten healthy volunteers were recruited for the study. The study was performed in compliance with all applicable institutional and other requirements of the University of Johannesburg (UJ). The UJ Higher Degrees and Ethics Committees approved the study. Volunteers were informed about the nature and purpose of the study and had to give informed consent before inclusion. Exclusion criteria were ocular disease, contact lens wearers and ocular surgery (including refractive or laser surgery). All subjects had healthy, normal eyes as verified by slit lamp examination and direct ophthalmoscopy. All examinations took place on the same day with a 5- to 10-minutes interval between the measurements of the two different instruments. The order in which the instruments were used was randomized. A coin was flipped to determine which instrument was used first (head was for the autokeratometer while tails was for the Pentacam).

The Pentacam system consists of the Pentacam itself and a computer. The software is almost fully automated. After each subject's data was entered, the program was changed to imaging mode. Each subject sat on a chair in front of the camera and placed the chin on the chin rest and pressing the forehead lightly onto the forehead rest. Each subject was asked to open both eyes and look into the black spot in the middle of the blue fixation beam of the instrument. Meanwhile, the researcher observed the image of the eye on the computer screen, with the machine automatically marking the pupil centre, pupil edge and the corneal apex. The image was focused and centered manually by moving the Pentacam in the respective directions (using arrows displayed on the screen indicating the direction the researcher should move the joystick of the camera in the horizontal, vertical and longitudinal axes). The Pentacam automatic release mode was used. In this mode, measurements begin automatically when correct focus and alignment with the corneal apex are achieved. In less than two seconds, the rotating camera took 25 slit images of the anterior eye segment. Each set of measurements (25 cross-sectional scans of the cornea) took about a minute, and 43 successive measurements or sets for the right eye of each subject were obtained. The reason for 43 measurements was to allow for the possible removal of a limited number of outliers. A minimum size of 40 sets per subject was considered necessary. For one to be confident that an instrument provides accurate and repeatable measures of keratometry, multiple measurements must be taken. Between each set of measurements subjects were asked to remove their heads momentarily from the machine when it was processing the measured corneal sections. Thus it required about 50 minutes per subject to obtain all the necessary data for the Pentacam.

A Nidek ARK-700 autokeratometer was also used to obtain 43 successive central readings on the right eye of each subject. Each subject placed their chin on the instrument's chin rest and pressed their forehead lightly onto the forehead rest. Each subject was asked to open both eyes and look at the target, namely a yacht on the ocean, inside the autokeratometer. The researcher saw the image of the cornea on the screen and brought the image into alignment and centralized it within the central measurement circle on the screen. When satisfactory alignment and focusing had been achieved the measurement button was pressed and the corneal radii of curvatures in the principal meridians were printed. The subject was asked to briefly remove their head and then the autokeratometer was refocused and the next measurement was printed. This process was repeated until the 43 successive measurements and readings were printed. The process required about 20 minutes per subject. Thus the total examination time was about 70 minutes per subject, approximately 50 minutes for Pentacam and 20 minutes for the autokeratometer.

Statistical analysis

For each subject, the samples ($N = 43$ each) of principal radii of curvature from the Pentacam and from the autokeratometer were converted to dioptric power matrices using a refractive index of 1.375 (that is, the refractive index of the typical cornea rather than the standard keratometric index of 1.3375). The data were analysed using mathematical methods developed by Harris[13-21] and software developed by Harris and Malan[22] and modified by Rubin.[23] The methods convert sphero-cylindrical powers in clinical notation into dioptric power matrices. Stereo-pair scatter plots, variance-covariance profiles of dioptric power and hypotheses on variances and covariances, and on mean dioptric powers were determined for the Pentacam and the autokeratometer samples.

The analysis begins with the dioptric power matrix $\mathbf{F}$ and its coordinate vector $\mathbf{f}$. In its most general form the dioptric power matrix can be expanded as

$$\mathbf{F} = F_\mathrm{I}\mathbf{I} + F_\mathrm{J}\mathbf{J} + F_\mathrm{K}\mathbf{K} + F_\mathrm{L}\mathbf{L} \tag{1}$$

where

$$\mathbf{I} = \begin{pmatrix} 1 & 0 \\ 0 & 1 \end{pmatrix}, \; \mathbf{J} = \begin{pmatrix} 1 & 0 \\ 0 & -1 \end{pmatrix}, \; \mathbf{K} = \begin{pmatrix} 0 & 1 \\ 1 & 0 \end{pmatrix} \text{and } \mathbf{L} = \begin{pmatrix} 0 & -1 \\ 1 & 0 \end{pmatrix} \tag{2}$$

For the common symmetric case (the kind commonly encountered in optometry) the antisymmetric component ($F_L\mathbf{L}$) vanishes and equation 1 reduces to

$$\mathbf{F} = F_\mathrm{I}\mathbf{I} + F_\mathrm{J}\mathbf{J} + F_\mathrm{K}\mathbf{K} \tag{3}$$

Symmetric powers $\mathbf{F}_i$ are plotted on three mutually orthogonal axes representing stigmatic ($F_\mathrm{I}\mathbf{I}$), ortho-antistigmatic ($F_\mathrm{J}\mathbf{J}$) and oblique antistigmatic($F_\mathrm{K}\mathbf{K}$) powers respectively. In these three-dimensional graphs each point represents a distinct power. Each symmetric power can be written as a coordinate vector[18-21, 24]

$$\mathbf{f} = (F_\mathrm{I} \; F_\mathrm{J} \; F_\mathrm{K})^{\,t} \tag{4}$$

For a sample of powers, an arithmetic mean of the dioptric power matrices or of the coordinate vectors can be determined and the variation of dioptric power is described by a 3x3 symmetric variance-covariance matrix $\mathbf{S}$ with six distinct entries

$$\mathbf{S} = \begin{pmatrix} s_\mathrm{II} & s_\mathrm{IJ} & s_\mathrm{IK} \\ s_\mathrm{JI} & s_\mathrm{JJ} & s_\mathrm{JK} \\ s_\mathrm{KI} & s_\mathrm{KJ} & s_\mathrm{KK} \end{pmatrix} \tag{5}$$

where the diagonal entries s_II, s_JJ and s_KK are the variances and the off-diagonal entries s_IJ, s_IK and s_JK are the covariances.

Results

Table 1 provides various statistics for a single subject (Subject 1), and the means both in conventional sphero-cylindrical form and as a dioptric power matrix with outliers (Table 1a) and when two outliers had been removed (Table 1b). Figure 1 shows stereo-pair scatter plots of the dioptric powers of the autokeratometric measurements with (*a*) outliers and (*b*) when the outliers had been removed and also for the Pentacam measurements (*c*) of the cornea, each with its associated 95% distribution ellipsoid. The origin of each plot is at the applicable sample mean (given in Table 1). Figure 2 shows plots comparing the autokeratometric and Pentacam measurement with (*a*) and without (*b*) outliers. Two outermost points (see Figure 1a) seem to be somewhat removed from the rest. The Mahalanobis distances were determined for all points and the two points with the greatest Mahalanobis distances were regarded as outliers. Once the outliers were removed the shape, orientation and distribution ellipsoids are similar and overlapping; that is, the anterior corneal powers were quite similar. The origins in Figures 1a and 1b are at the mean powers of the cornea. Outliers represent atypical behaviour of the eye and are not due to inaccurate autokeratometer measurement. Something occurred, such as a sudden change in eye position or movement or momentary corneal change due to lid movement during blinking resulting in such measurements. Evaporation of the tear layer may also sometimes be an important factor.

Table 1. Statistics for the right eye of a single subject (Subject 1) for the samples of autokeratometry and Pentacam measurements are given. The mean powers, variance-covariance matrices and the volumes of the ellipsoids of constant probability density containing an estimated 95% of the population of measurements with (a) and without (b) outliers are indicated.
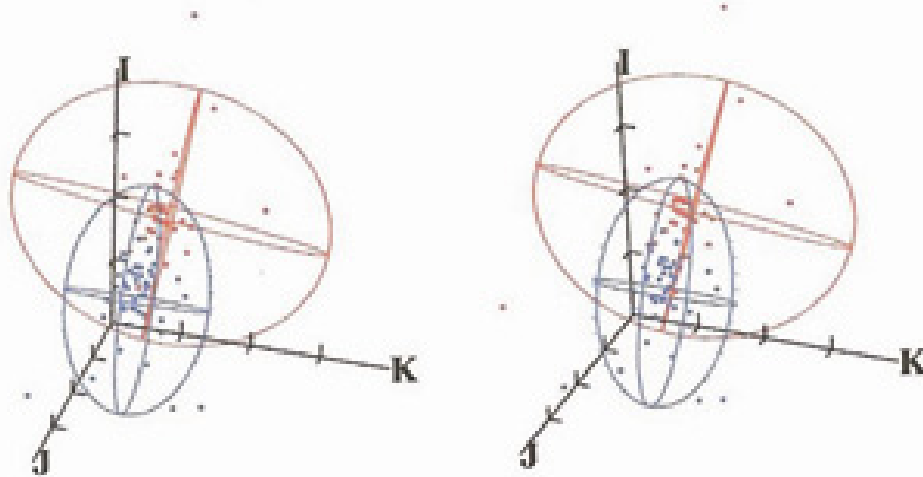
(a)	Autokeratometer	Pentacam
Means (D) Conventional Scientific	$43.61 - 0.65 \times 79$ $43.30\mathbf{I} - 0.30\mathbf{J} + 0.12\mathbf{K}$	$43.19 - 0.44 \times 86$ $42.97\mathbf{I} - 0.22\mathbf{J} + 0.03\mathbf{K}$
Variance-covariance Matrices (D^2)	$\mathbf{S} = \begin{pmatrix} 0.0159 & -0.0105 & -0.0084 \\ -0.0105 & 0.0158 & -0.0081 \\ -0.0084 & -0.0081 & 0.0364 \end{pmatrix}$	$\mathbf{S} = \begin{pmatrix} 0.0166 & -0.0065 & 0.0003 \\ -0.0065 & 0.0068 & 0.0006 \\ 0.0003 & 0.0006 & 0.0090 \end{pmatrix}$
Volume (D^3)	0.30	0.20

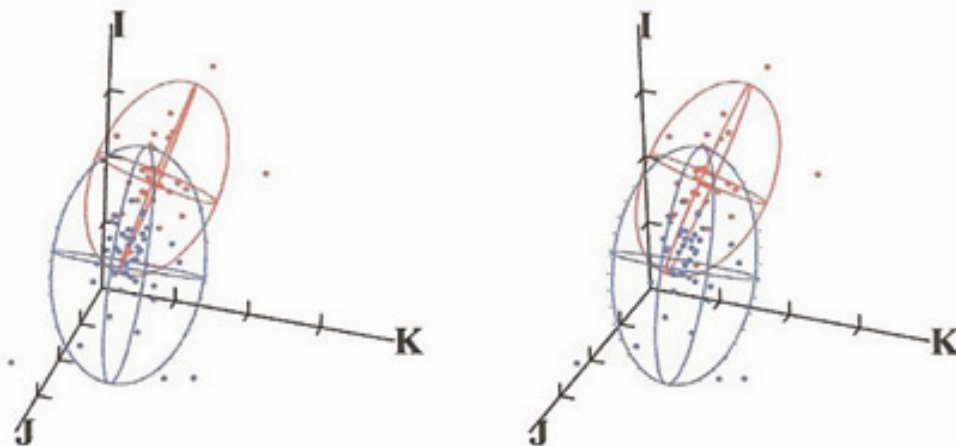| (b)	Autokeratometer	Pentacam
Means (D) Conventional Scientific	$43.60 - 0.62 \times 81$ $43.29\mathbf{I} - 0.30\mathbf{J} + 0.10\mathbf{K}$	$43.19 - 0.44 \times 86$ $42.97\mathbf{I} - 0.22\mathbf{J} + 0.03\mathbf{K}$
Variance-covariance matrices (D^2)	$\mathbf{S} = \begin{pmatrix} 0.0080 & -0.0067 & 0.0004 \\ -0.0067 & 0.0086 & -0.0017 \\ 0.0004 & -0.0017 & 0.0058 \end{pmatrix}$	$\mathbf{S} = \begin{pmatrix} 0.0166 & -0.0065 & 0.0003 \\ -0.0065 & 0.0068 & 0.0006 \\ 0.0003 & 0.0006 & 0.0090 \end{pmatrix}$
Volume (D^3)	0.12	0.20

(a)

(b)

(c)
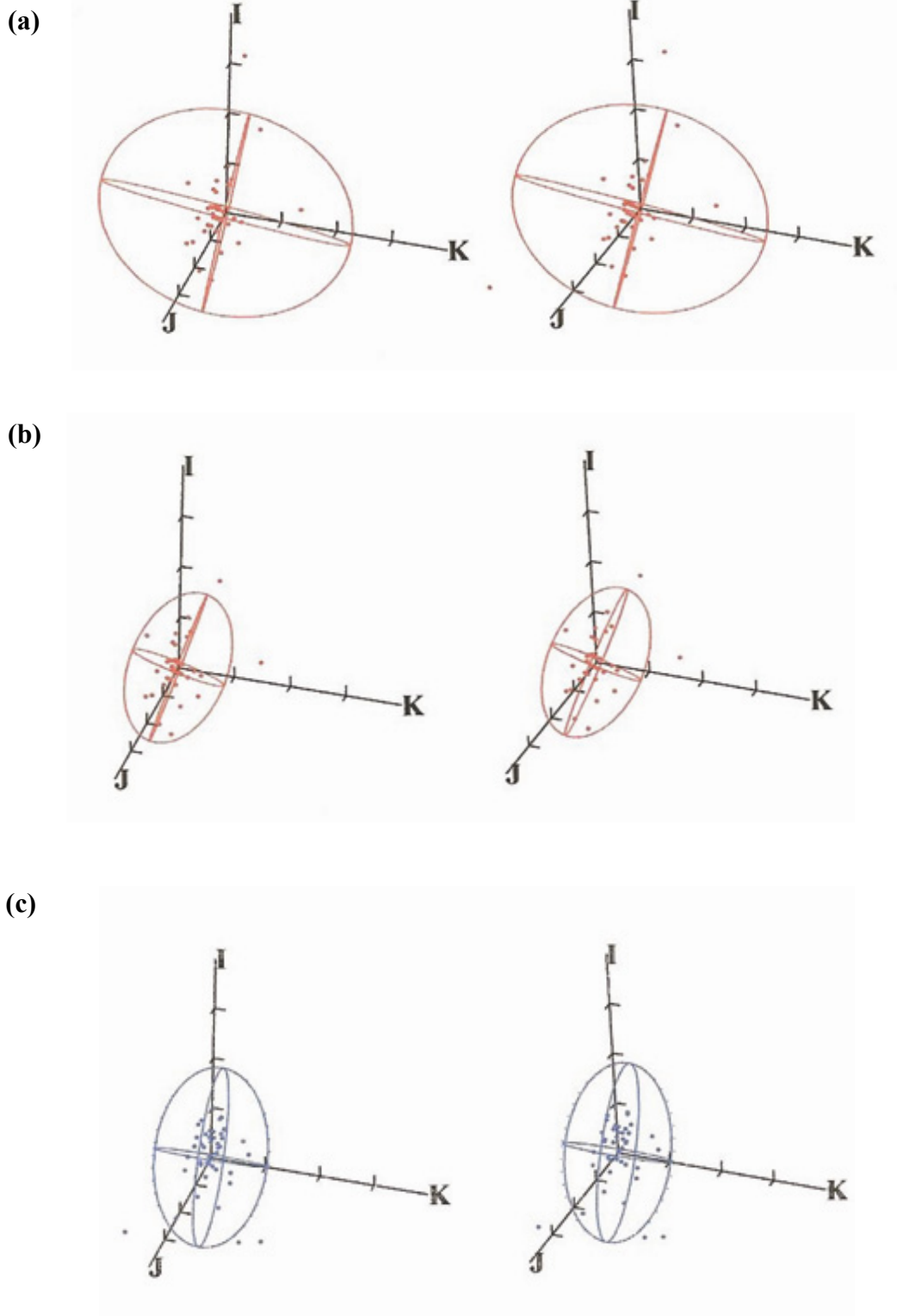
Figure 1. Stereo-pair scatter plots for Subject 1 in symmetric power space representing autokeratometry measurements (*a*) with and without (*b*) two outliers and Pentacam measurements (*c*). The three mutually orthogonal axes represent the scalar $F_I I$, ortho-antistigmatic $F_J J$ and oblique antistigmatic $F_K K$ components of the powers. The origin of each stereo-pair represents the applicable sample mean (see Table 1). Each dot represents one measurement of the anterior keratometry (or corneal power) and tick intervals are $0.25I$, $0.25J$ and $0.25K$ respectively.

(a)

(b)

Figure 2. Two stereo-pair scatter plots for Subject 1 showing the keratometric measurements obtained using an autokeratometer (red) and Pentacam (blue) with (**a**) and without two outliers (**b**). For both plots the origin of the axes is set at the power 43 D (in conventional terms) and the tick interval is 0.25 D. Removal of the outliers reduces the volume of the red ellipsoid and changes its orientation.
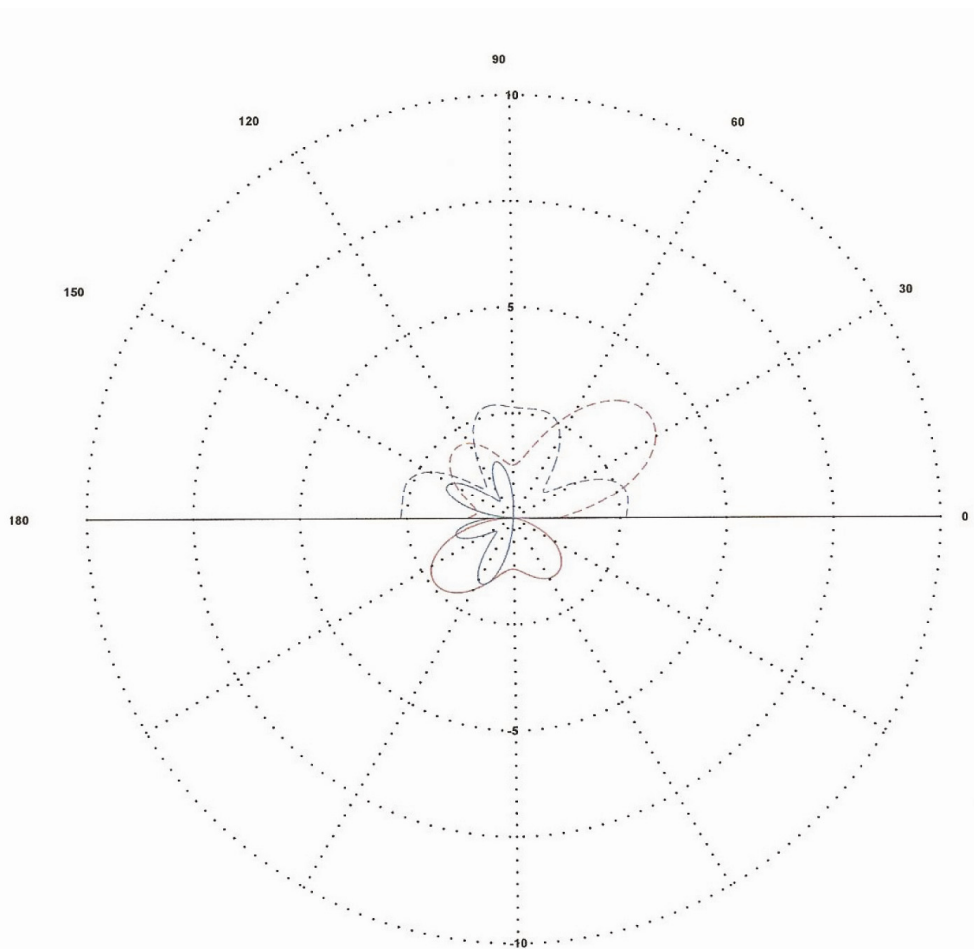
(a)
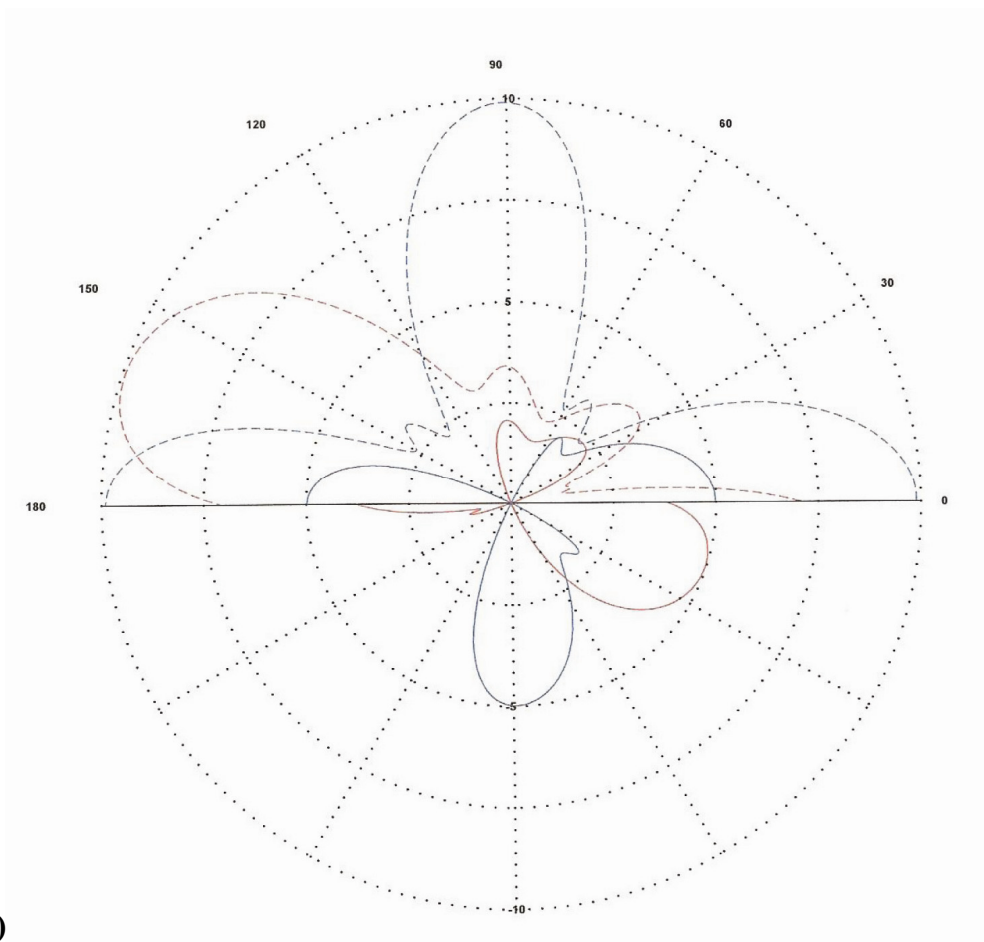
**(b)**
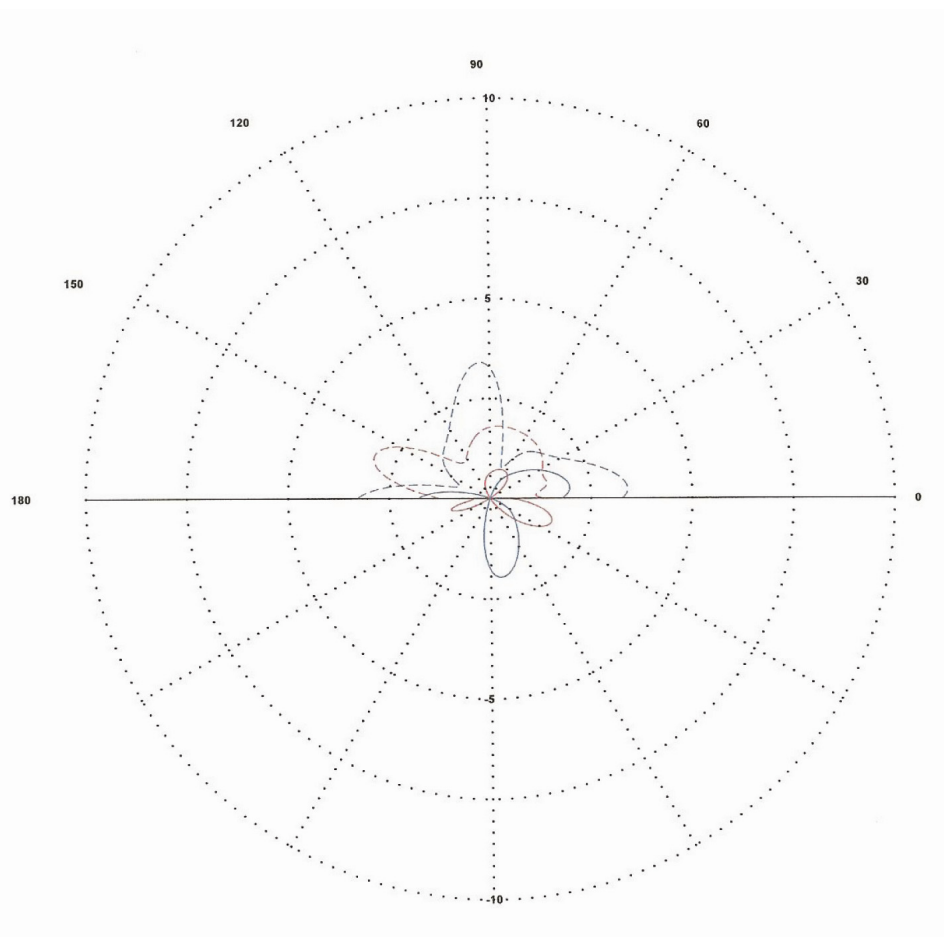
(c)

Figure 3. Polar plots of 1/3 skew ness and kurtosis for meridians 0 to 180° for Subject 1 for the autokeratometer with (*a*) and without (*b*) two outliers are indicated. The polar plot for the sample for the Pentacam (*c*) is also provided. Solid lines represent skewness where red (= f_{11}) and blue (= f_{21}). Dashed lines represent kurtosis where red (= f_{11}) and blue (= f_{21}). Normal distributions have a skewness of 0 and a $\frac{1}{3}$ kurtosis of 1. Once the outliers were removed the data was more normally distributed (compare (*a*) and (*b*)). Figures 3(*b*) and 3(*c*) indicate that the samples for both instruments were relatively normally distributed once outliers were removed.

(a)

(b)

(c)
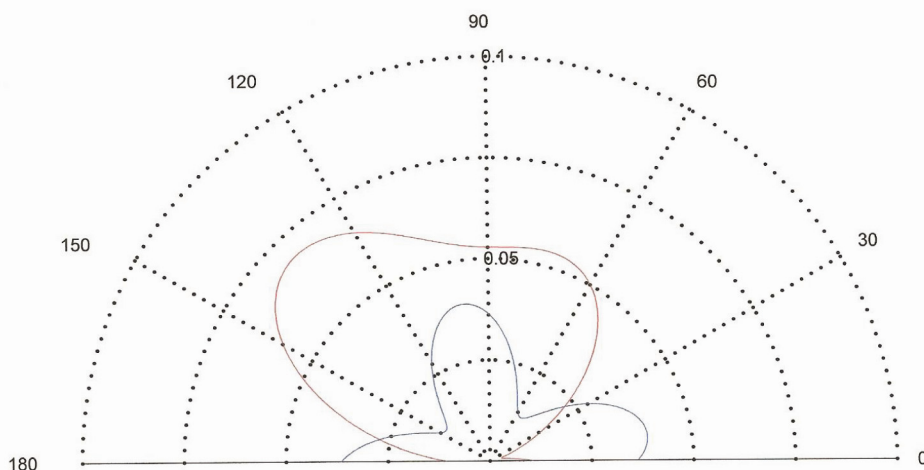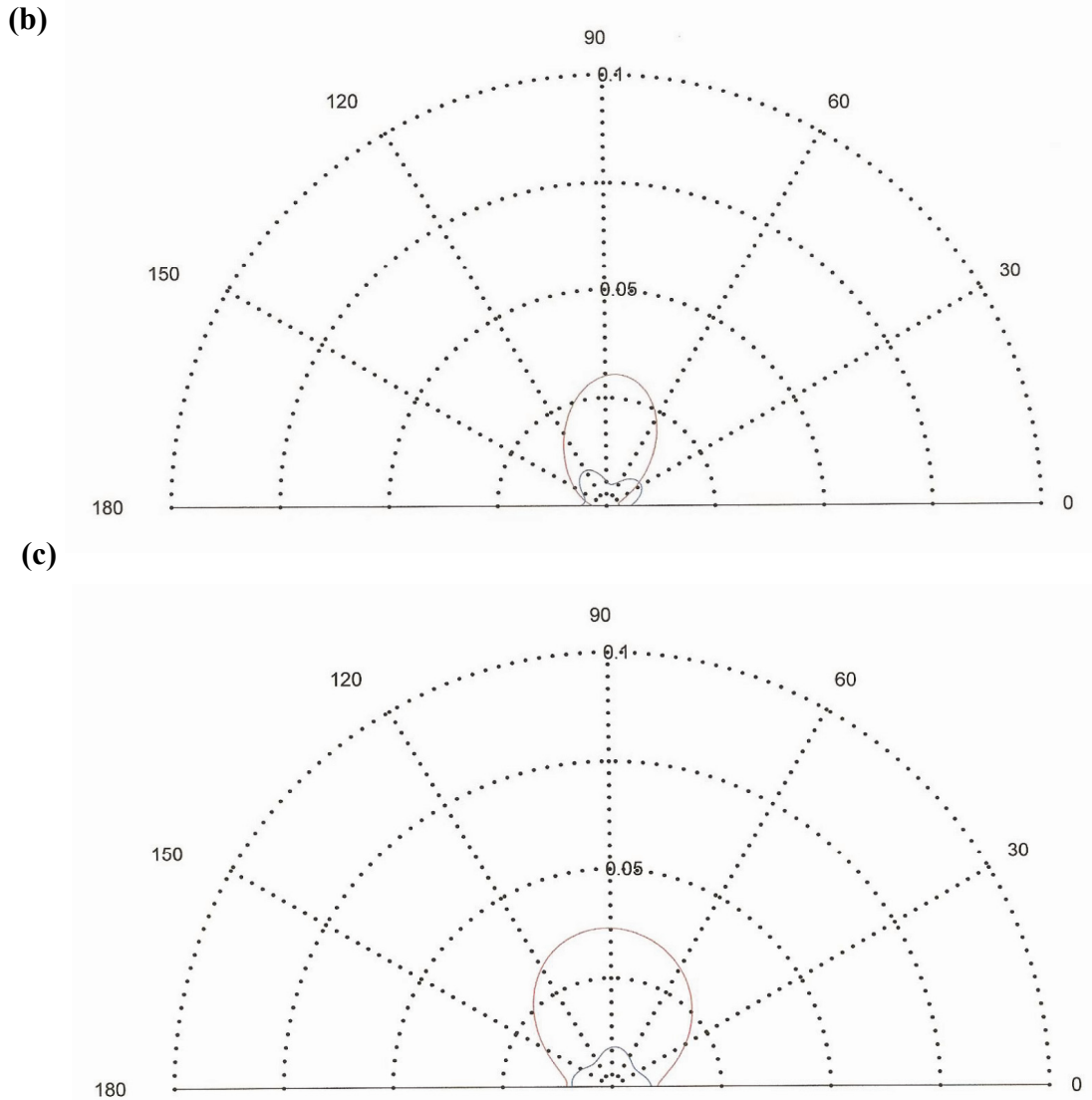
Figure 4. Polar profiles of variance with (*a*) and without (*b*) two outliers for Subject 1 for the autokeratometer and (*c*) for the Pentacam. The radial coordinate has units D^2. The scale was kept constant to accommodate the curves of graph 4(*a*). Once the outliers were removed the variances for the autokeratometric samples decreased markedly. Figures 3(*b*) and (*c*) indicate that the measurements were not very variable irrespective of instrument concerned. The red and blue lines are the curvital and torsional varances, respectively.

Polar profiles provide a graphical presentation of f_{11} and f_{21} (of all $\mathbf{F}_i$) for each meridian from 0 to 180°. Figure 3 shows the profiles of skewness and 1/3 kurtosis with (*a*) outliers and without (*b*) two possible outliers. With possible outliers included there is negative skewness for f_{11} along 160° and along 90° for f_{21}. There is leptokurtosis along 160° for f_{11} and along 90° and 180° for f_{21}. For the Pentacam measurements there is leptokurtosis along 40° for f_{11} and along 20°, 90° and 160° for f_{21}. There is a negative skewness for f_{11} along 40° and along 20° and 60° for f_{21}. Figure 4 presents polar profiles of curvital (f_{11}) and torsional (f_{21}) variance. Such profiles indicate the meridian(s) in which the components of power have maximum or minimum variation.

For this subject, a statistically significant difference was observed between the variances and covariances of the autokeratometer and the Pentacam samples. Table 2 presents the results of hypothesis tests done on the variances and covariances. The test was conducted at a 95% level of confidence, the critical values being 2.72 for means and 12.592 for variance-covariances at $p = 0.05$. The means were also significantly different but in Table 1a the differences can be seen to be very minor from a clinical perspective.

Table 2. The results of the hypothesis tests for the variance-covariance matrices and means for Subject 1 are included. The level of significance is *p* = 0.05. The null hypothesis (*H*ₒ) of equality is rejected if the test statistic is larger than the critical value.

	Critical value	Test statistic	Test statistic
With outliers Means	2.72	$F_{(\alpha, 3, 80)}$	$w = 73.05$
Variances and covariances	12.592	$\chi^2_{(\alpha, 6)}$	$\mu = 51.52$
Outliers removed Means	2.72	$F_{(\alpha, 3, 80)}$	$w = 71.91$
Variance and covariances	12.592	$\chi^2_{(\alpha, 6)}$	$\mu = 23.422939$

Discussion

In this study, we compared keratometric measurements obtained using the Nidek ARK-700 autokeratometer and Pentacam 70700. Of special concern was to show how Pentacam measurements taken from normal corneas compared to those from the more commonly clinically used autokeratometric method. Although numerous studies[6-12] have been performed to compare different pachymetry methods, to our knowledge this is the first study evaluating the keratometry measurements of the Pentacam in normal eyes. Currently, articles about pachymetry and central corneal thickness measurements between the Pentacam and other approaches have been published.[6-12] But to our knowledge, a comparison between autokeratometry and Pentacam using the multivariate methods utilized here has not been conducted before.

Stereo-pair scatter plots (Figures 1 and 2) show in dioptric power space all measurements from the two instruments on this single right eye of Subject 1. These plots make it easier to assess the magnitude of dissimilarities, observe outliers and observe relevant trends in data. Results for the two instruments were markedly similar, or at least so for this particular subject. Although not included here in detail similar findings were found for the other nine subjects, but such analysis is ongoing and will be included in future papers.

The volume contained within the 95% distribution ellipsoid for the autokeratometer is 0.30 D^3 with an outlier and 0.20 D^3 for the Pentacam. When outliers were removed, the volume for the autokeratometer sample was reduced to 0.12 D^3 and the direction of the spread of measurements also changed (and became more similar to that of the ellipsoid for the Pentacam sample). Since the volume was smaller for the autokeratometer after the outliers were removed, we can be more confident about the mean keratometric state (see Table 1b) obtained for the eye.

Although the variances and covariances (and means) were statistically different for measurements for the autokeratometer and Pentacam, clinically the differences were negligible. Therefore, the two instruments provide similar results for the anterior corneal radii and powers. The differences could be due to the differences in regions of cornea imaged by each device and that the two devices use different modes of operation.

Conclusion

Both autokeratometers and the Pentacam can be used to obtain keratometric measurements of the anterior cornea. For at least this subject the differences between these two instruments could be regarded as being within a clinically insignificant error range. But further work is currently ongoing to verify whether the keratometric measurements by these two instruments can be used interchangeably in other eyes, and especially in eyes with conditions such as keratoconus for instance.

Acknowledgement

References

1. Bennett AG and Rabbetts RB. What radius does the conventional keratometer measure? *Ophthal Physiol Opt* 1991 **11** 239-247.
2. Tunnacliffe AH. *Introduction to Visual Optics*. 4th ed. Britain: Association of British Dispensing Opticians, 2001 33.
3. Cronje S and Harris WF. Short-term keratometric variation in the human eye. *Ophthal Physiol Opt* 1997 **74** 420-424.
4. Mathebula SD. Relation between corneal and total astigmatism. *S Afr Optom* 1998 **57** 105-108.
5. *Pentacam Instrument Manual: measurement and evaluation system for the anterior segment of the eye*. Oculus 70700: Wetzlar, Germany, March 2005.
6. Buehl W, Stajanac D, Sacu S, Drexter W and Findl O. Comparison of three methods of measuring corneal thickness and anterior chamber depth. *Am J Ophthalmol* 2006 **141** 7-12.
7. Lackner B, Schmidinger G and Skorpik C. Validity and repeatability of anterior chamber depth measurements with Pentacam and Orbscan. *Optom Vis Sci* 2005 **82** 858-861.
8. Lackner B, Schmidinger G, Pieh S, Funovics MA and Skorpik C. Repeatability and reproducibility of central corneal thickness measurement with Pentacam, Orbscan and Ultrasound. *Optom Vis Sci* 2005 **82** 892-899.
9. Rabsilber TM, Khoramnia R and Auffart GU. Anterior chamber measurements using Pentacam rotating Scheimpflug camera. *J Cataract Refract Surg* 2006 **32** 456-459.
10. O'Donnell C and Maldonado-Codina C. Agreement and repeatability of central thickness measurement in normal corneas using ultrasound pachymetry and the Oculus Pentacam. *Cornea* 2005 **24** 920-924.
11. Tong L, Wong EH, Chan YH and Balakrishnan V. Agreement between Scheimpflug photography and A-scan ultrasonography in anterior segment ocular measurements in children. *Optom Vis Sci* 2003 **80** 529-534.
12. Elbaz U, Barkana Y, Gerber Y, Avni I and Zadok D. Comparison of different techniques of anterior chamber depth and keratometric measurements. *Am J Ophthalmol* 2007 **143** 48-53.
13. Harris WF. A simplified rational representation of dioptric power. *Ophthal Physiol Opt* 1989 **9** 455.
14. Harris WF. A measure of vision. *S Afr Optom* 1990 **49** 9-15.
15. Harris WF. Direct, vec and other squares, and sample variance-covariance of dioptric power. *Ophthal Physiol Opt* 1990 **10** 72-80.
16. Harris WF. Representation of dioptric power in Euclidean 3-space. *Ophthal Physiol Opt* 1991 **11** 130-136.
17. Harris WF. Testing hypotheses on dioptric power. *Optom Vis Sci* 1992 **69** 835-845.
18. Harris WF. Graphical representation of symmetric dioptric power and the concepts of stigmatic, antistigmatic and antistigmatic power. *S Afr Optom* 2002 **61** 126-134.
19. Harris WF. Inner product spaces of dioptric power and of fundamental and derived properties of optical systems. *S Afr Optom* 2003 **62** 114-118.
20. Harris WF and Rubin A. Error cells for spherical powers in symmetric dioptric power space. *Optom Vis Sci* 2005 **82** 633-636.
21. Harris WF. Dioptric power: its nature and its representation in three- and four-dimensional space. *Optom Vis Sci* 1997 **74** 349-366.
22. Malan DJ. Dioptric power data analysis: computer implementation of graphical methods with clinical examples. *S Afr Optom* 1993 **52** 84-90.
23. Rubin A. Statistical analysis of autorefractor measurements on a single subject. *S Afr Optom* 1993 **52** 91-97.
24. Thibos LN, Wheeler W and Horner D. Power vectors: an application of Fourier analysis to the description and statistical analysis of refractive error. *Optom Vis Sci* 1997 **74** 367-375.
25. Raasch T. Clinical refraction in the three-dimensional dioptric space revisit. *Optom Vis Sci* 1997 **74** 376-380.
26. Deal FC and Toop J. Recommended coordinate systems for thin spherocylinderical lenses. *Optom Vis Sci* 1993 **70** 409-413.
27. Harris WF. Coordinate systems and vector spaces for lenses. *Optom Vis Sci* 1994 **71** 145-147.